The Abdus Salam
International Centre for Theoretical Physics

United Nations
Educational, Scientific
and Cultural Organization

International Atomic
Energy Agency

SMR 1673/44

AUTUMN COLLEGE ON PLASMA PHYSICS

5 - 30 September 2005

Acceleration of Plasma Flows Due to Magneto-Fluid Coupling

N. Shatashvili

Plasma Physics Department, Tbilisi State University
Georgia

Acceleration of Plasma Flows Due to Magneto-Fluid Coupling

Nana L. Shatashvili
Plasma Physics Department,
Tbilisi State University, Georgia

In collaboration with

S.M. Mahajan, Z. Yoshida, R. Miklaszewski,

K.I. Nikol'skaya, S. Ohsaki,

S.V. Mikeladze, K.I. Sigua

High-energy particle acceleration is observed in a diverse variety of laboratory devices as well as astrophysical sites ranging from the terrestrial aurorae to the most distant quasars.

In astrophysical sites particle acceleration is a fairly common channel for the release of large-scale kinetic, rotational and magnetic energy.

Physical mechanisms include electrostatic acceleration, stochastic processes and diffusive shock energization.

The overall acceleration efficiency is controlled by the low-energy particle injection.

It is often observed **the acceleration of plasma flows** (creation of stellar winds, variety of jets, zonal flows in TOKAMAK-s and etc.) both in laboratory and space plasmas.

R.D. Blandford. ApJ (1994), 90, 515.

Sources of free energy for particle acceleration:

"Source" - agency whose energy is permanently decreased in order to power the acceleration.

- **Bulk kinetic energy of fluid motion in the form of shock front** - often consequence of an explosion (supernova, coronal mass ejection); relativistic shocks as may take the form of a standing shock as in the termination shock of the Crab pulsar wind, or may travel at ultra-relativistic jets of extragalactic radio sources.
- **Rotational energy** - invoked in Jupiter-Jo system; radio pulsars; black holes in both AGN and stellar binary systems.
- **Magnetic energy** - Earth's magnetotail; solar flares; is conjectured to occur in coronal regions above accretion disks, and etc.

- Recent observations, strongly fortified by improved measuring and interpretive capabilities, have convincingly demonstrated that **the solar corona is a highly dynamic arena replete with multi-species multiple–scale spatiotemporal structures**. E.g. Aschwanden, Poland & Rabin, 2001, ARA&A.
- A major new advance is the discovery that **strong flows are found everywhere in the low atmosphere — in the sub-coronal (chromosphere) as well as in coronal regions**.

  See e.g. Schrijver et al. 1999, Solar Physics; Wilhelm 2000, A&A; Winebarger, DeLuca and Golub 2001, APJ; Aschwanden et al. 2001, ARA&A; Aschwanden 2001, APJ; Seaton e et al. 2001, APJ; Winebarger et al. 2002, APJ and references therein.
- Equally important: **the plasma flows may complement the abilities of the magnetic field in the creation of the amazing richness observed in the coronal structures**.

  See e.g. Orlando, Peres and Serio 1995, A&A; Nikol'skaya and Valchuk, 1998, Geomagn. Aeron.; Mahajan et al. 1999, 2001, PoP; Adv. Space. Res. Vol.30(3),2002.

Challenge – to develop a theory of flow generation/acceleration in the lower atmosphere.

Evolution of Corona Cartoon

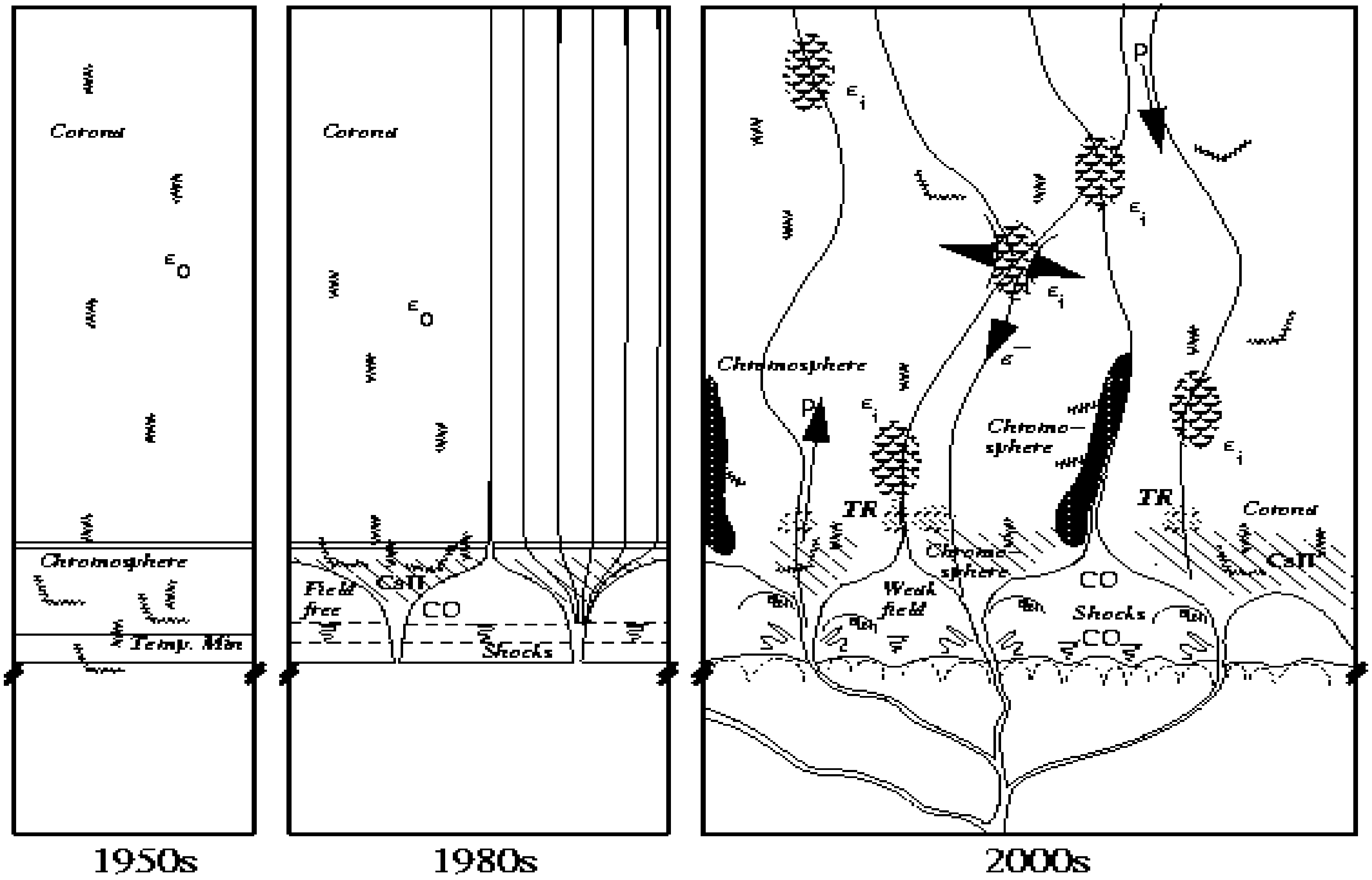

Evolution of corona cartoon: gravitationally stratified layers in the 1950s (left); vertical flux tubes with chromospheric canopies (1980s, middle); fully inhomogeneous mixing of photospheric, chromospheric, TR and coronal zones by such processes as heated upflows, cooling downflows, interminent heating (ε), nonthermal electron beams (e), field line motions and reconnections, emission from hot plasma, absorption and scattering in cool plasma, acoustic waves, shock waves (right). (**from Shrijver 2001**).

Associating the traditional layers with temperature rather than height is only a little better.

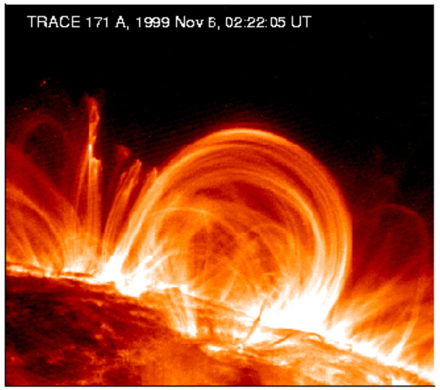

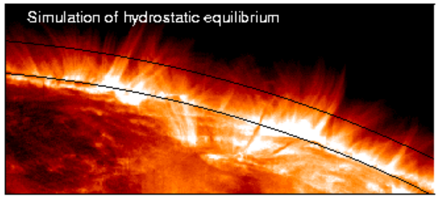

Fine Structure of Solar Atmosphere:
Co-existed varying scale different temperature closed field structures
(Aschwanden, Schrijver and Alexander, 2000)

Plasma β in the solar atmosphere for two assumed field strengths, 100G and 2500G
(Courtesy of G. Allen Gary)

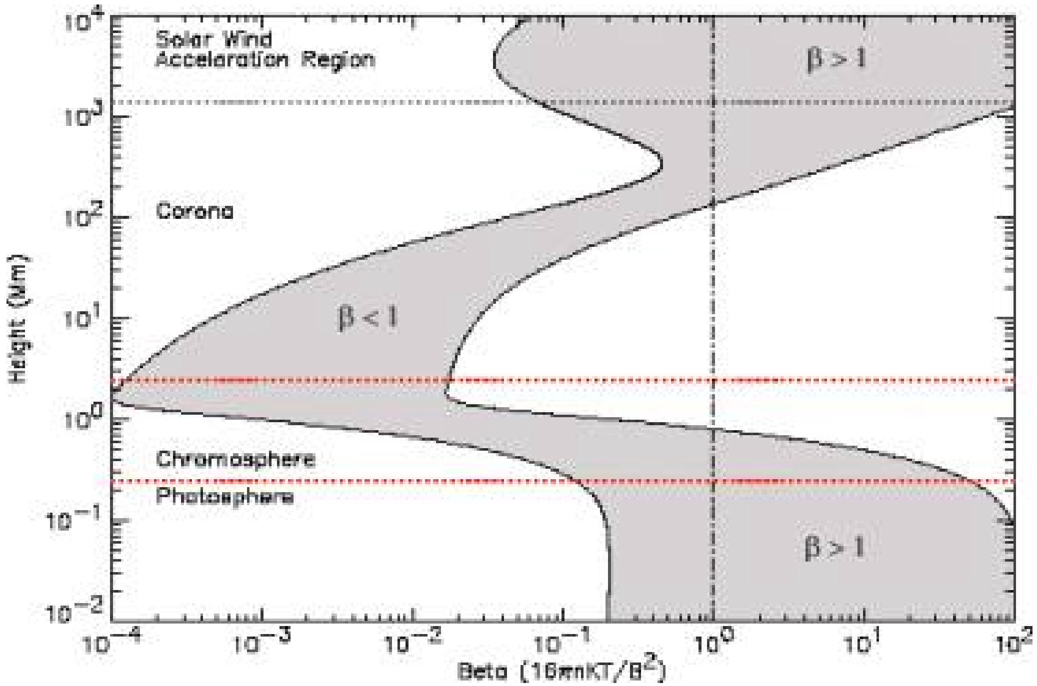

Acceleration of Plasma Flows

The most obvious process for acceleration (rotation is ignored):

- **the conversion of magnetic**
- **and/or the thermal energy**

  to plasma kinetic energy.

Magnetically driven transient but **sudden** flow–generation models:

- **Catastrophic models**
- **Magnetic reconnection models**
- **Models based on instabilities**

Quiescent pathway:

- *Bernoulli mechanism converting thermal energy into kinetic*
- General magnetofluid rearrangement of a relatively constant kinetic energy: going from an initial high density–low velocity to a low density–high velocity state.

Magneto-fluid Coupling

$\mathbf{V}$ — the flow velocity field of the plasma
Total current $\mathbf{j} = \mathbf{j}_0 + \mathbf{j}_s$. $\mathbf{j}_s$ – self-current (generates $\mathbf{B}_s$).
Total (observed) magnetic field — $\mathbf{B} = \mathbf{B}_0 + \mathbf{B}_s$.

The stellar atmosphere is finely structured.
Multi-species, multi-scales. Simplest – two-fluid approach.
Quasineutrality condition: $n_e \simeq n_i = n$

Electron and proton flow velocities are different.

$$\mathbf{V}_i = \mathbf{V}, \qquad \mathbf{V}_e = (\mathbf{V} - \mathbf{j}/en)$$

Nondissipative limit: electrons frozen in electron fluid; ion fluid (finite inertia) moves distinctly.
The kinetic pressure: $p = p_i + p_e \simeq 2\,nT, \qquad T = T_i \simeq T_e.$
Heating due to the viscous dissipation of the flow vorticity:

$$\left[\frac{d}{dt}\left(\frac{m_i \mathbf{V}^2}{2}\right)\right]_{\text{visc}} = -m_i n \nu_i \left(\frac{1}{2}(\nabla \times \mathbf{V})^2 + \frac{2}{3}(\nabla \cdot \mathbf{V})^2\right). \qquad (1)$$

Quasi-equilibrium Approach

Model: recently developed magnetofluid theory.

Mahajan & Yoshida, 1998, PRL, 81, 4863.

Assumption: at some distance there exist fully ionized and magnetized plasma structures such that the quasi–equilibrium two–fluid model will capture the essential physics of flow acceleration.

Simplest two–fluid equilibria: $T = \mathrm{const} \longrightarrow \mathrm{n}^{-1}\nabla \mathrm{p} \rightarrow \mathrm{T}\nabla \ln \mathrm{n}.$
Generalization to homentropic fluid: $p = \mathrm{const}{\cdot}\mathrm{n}^{\gamma}$ is straightforward.
The **dimensionless equations**: Mahajan et al. 2001, Phys. Plasmas, 8, 1340

$$\frac{1}{n}\nabla \times \mathbf{b} \times \mathbf{b} + \nabla\left(\frac{r_{A0}}{r} - \beta_0 \ln\, n - \frac{V^2}{2}\right) + \mathbf{V} \times (\nabla \times \mathbf{V}) = 0, \quad (2)$$

$$\nabla \times \left[\left(\mathbf{V} - \frac{\alpha_0}{n}\nabla \times \mathbf{b}\right) \times \mathbf{b}\right] = 0, \quad (3)$$

$$\nabla \cdot (n\mathbf{V}) = 0, \quad (4)$$

$$\nabla \cdot \mathbf{b} = 0, \quad (5)$$

Normalizations:
$n \to n_0$ – the density at some appropriate distance from surface,
$B \to B_0$ – the ambient field strength at the same distance
$|V| \to V_{A0}$ – Alfvén speed

Parameters:
$r_{A0} = GM/V_{A0}^2 R_0 = 2\beta_0\, r_{c0}$, $\alpha_0 = \lambda_{i0}/R_0$, $\beta_0 = c_{s0}^2/V_{A0}^2$,
c_{s0} — sound speed R_0 — the characteristic scale length,
$\lambda_{i0} = c/\omega_{i0}$ — the collisionless ion skin depth
are defined with $n_0,\ T_0,\ B_0$.

Hall current contributions are significant when
$\alpha_0 > \eta$, (η - inverse Lundquist number).
Important in: interstellar medium, turbulence in the early universe, white dwarfs, neutron stars, stellar atmosphere.
Typical solar plasma: condition is easily satisfied.

Hall currents modifying the dynamics of the microscopic flows/fields could have a profound impact on the generation of macroscopic magnetic fields (Mininni et al 2001,2003) and macroscopic flows (Mahajan et al 2002,2005).

The double Beltrami solutions are

$$\mathbf{b} + \alpha_0 \nabla \times \mathbf{V} = d\ n\ \mathbf{V}, \qquad \mathbf{b} = a\ n\ \left[\mathbf{V} - \frac{\alpha_0}{n} \nabla \times \mathbf{b}\right], \tag{6}$$

a **and** d **— dimensionless constants related to ideal invariants: The Magnetic and the Generalized helicities** (Mahajan & Yoshida 1998; Mahajan et al. 2001)

$$h_1 = \int (\mathbf{A} \cdot \mathbf{b})\ d^3x, \tag{7}$$

$$h_2 = \int (\mathbf{A} + \mathbf{V}) \cdot (\mathbf{b} + \nabla \times \mathbf{V}) d^3x. \tag{8}$$

Obeying the Bernoulli Condition

$$\nabla \left(\frac{2\beta_0 r_{c0}}{r} - \beta_0 \ln\ n - \frac{V^2}{2} \right) = 0, \tag{9}$$

Relating the density with the flow kinetic energy & gravity.

Eruptive and Explosive events, Flaring

$n = const$ The parameter change — sufficiently slow / adiabatic:
At each stage, the system can find its local DB equilibrium.
Slow evolution — the dynamical invariants: h_1, h_2, and the total (*magnetic plus the fluid*) energy E are conserved.
May a slowly evolving structure suffer a loss of equilibrium?

General solution of DB pair is expressed in terms of SB fields.

$$\boldsymbol{b} = C_\mu \boldsymbol{G}_\mu(\mu) + C_\lambda \boldsymbol{G}_\lambda(\lambda), \tag{10}$$

$$\boldsymbol{V} = \left(\frac{1}{a} + \mu\right) C_\mu \boldsymbol{G}_\mu(\mu) + C_\lambda \left(\frac{1}{a} + \lambda\right) \boldsymbol{G}_\lambda(\lambda). \tag{11}$$

The transition may occur in one of the following two ways:

1. When the roots (λ - large-scale, μ - short-scale) of the quadratic equation, determining the length scales for the field variation, go from being real to complex.
2. Amplitude of either of the 2 states ($C_{\mu/\nu}$) ceases to be real.

Ohsaki et al. ApJ 2001,2002

The three invariants h_1, h_2 and E provide the relations connecting 4 parameters $\lambda, \mu, C_\lambda, C_\mu$ that characterize the DB field. Ohsaki et al. ApJ, 2001,2002

Large scale λ – control parameter — observationally motivated choice.

We study the structure–structure interactions working with simple 2D Beltrami ABC field with periodic boundary conditions.

If λ and μ are complex, the equilibrium solution will have the spatially decaying (or growing) component initially.
We choose real λ, μ for quasi–equilibrium structures in atmospheres.

There are two scenarios of losing equiliubrium:
(1) Either of $C_{\mu/\nu}$ becomes zero (starting from positive values) for real $\lambda_{\mu/\nu}$,
(2) The roots $\lambda_{\mu/\nu}$ coalesce ($\lambda_\mu \leftrightarrow \lambda_\nu$) for real $\lambda_{\mu/\nu}$ and $C_{\mu/\nu}$.

Solar atmosphere: equilibria with vastly separated scales (for a variety of sub–alfvénic flows). (2) possibility is not of much relevance.

Flow Acceleration (N=const)

a) No catastrophe initial conditions
b) Catastrophe initial conditions

2D Beltrami ABC field with periodic boundary conditions

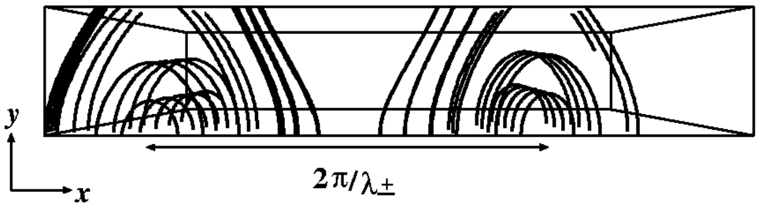

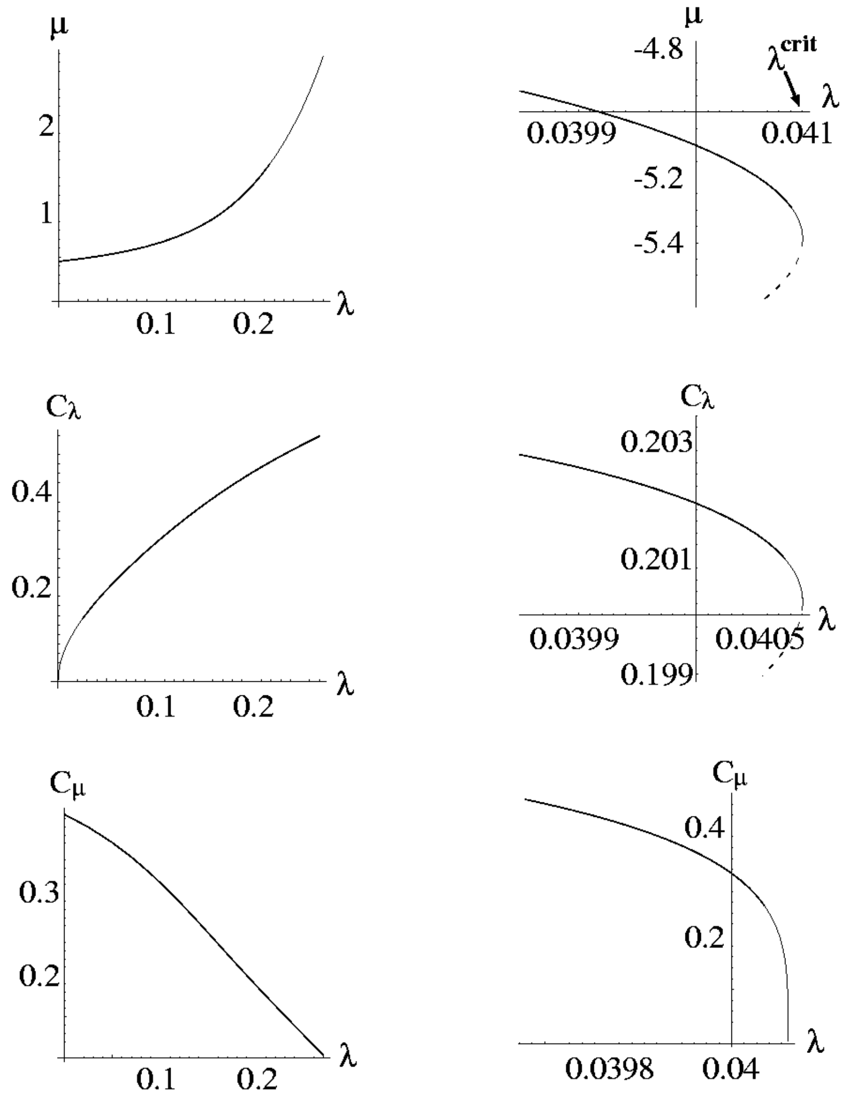

(a) (b)

Flow Acceleration (N=const)

a) No catastrophe initial conditions
b) Catastrophe initial conditions

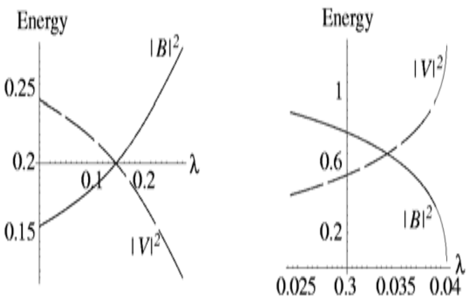

(a) (b)

Solar Atmosphere:
Almost all initial magnetic energy (short scale) is transferred to flow

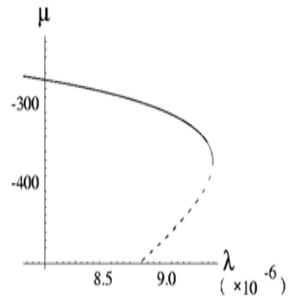

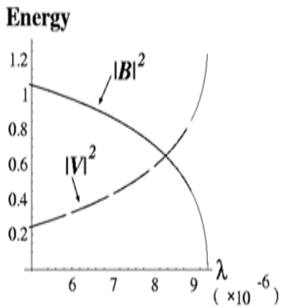

Root coalescence:
No separation between roots at the transition!

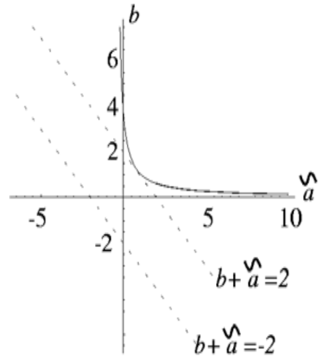

(a)

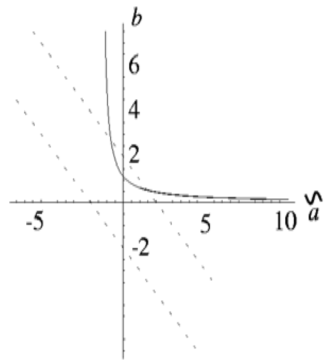

(b)

Results for uniform density case

- By modelling quasi–equilibrium, slowly evolving solar atmosphere structures as a sequence of DB magnetofiuid states the conditions for catastrophic changes leading to a fundamental transformation of the initial state are derived.
- When the total energy exceeds a critical energy the DB equilibrium suddenly relaxes to a single Beltrami state corresponding to the large macroscopic size.
- All of the short–scale magnetic energy is transformed to the flow kinetic energy.
- The proposed mechanism for the energy transformation work in all regions of Solar atmosphere with different dynamical evolution depending on the initial and boundary conditions for a given region.

Variational Principle $\Longrightarrow$ One can deal with any case:
constant density, constant temperature, or a given equation of state.

Non–uniform density case

Closed system (2), (6),(9) with $g(r) = r_{c0}/r \quad \Longrightarrow$

$$\frac{\alpha_0^2}{n}\nabla\times\nabla\times\mathbf{V} + \alpha_0\,\nabla\times\left[\left(\frac{1}{a\,n} - d\right) n\,\mathbf{V}\right] + \left(1 - \frac{d}{a}\right)\mathbf{V} = 0, \quad (12)$$

$$\alpha_0^2\nabla\times\left(\frac{1}{n}\nabla\times\mathbf{b}\right) + \alpha_0\,\nabla\times\left[\left(\frac{1}{a\,n} - d\right)\mathbf{b}\right] + \left(1 - \frac{d}{a}\right)\mathbf{b} = 0. \quad (13)$$

$$n = \exp\left(-\left[2g_0 - \frac{V_0^2}{2\beta_0} - 2g + \frac{V^2}{2\beta_0}\right]\right), \quad (14)$$

Caution: this time–independent set is not suitable for studying **primary** heating processes at lower heights (Mahajan et al. PoP 2001).

1D simulation - a variety of boundary conditions. Mahajan et al. ApJL 2002
The relevant dimension — the height "Z" from Stellar center.
Code limitations: α_0–s chosen for the simulation are much larger than their actual values ($\leq 10^{-8}$ for corona and sub–coronal regions).

Result: for small α_0 there exists some height where the density begins to drop precipitously with a corresponding sharp rise in the flow speed. The effect is stronger for low beta plasmas.

Bernoulli condition (14) yields an indirect estimate for the height at which the observed shock–formation may take place (for all α_0):

$$|\mathbf{V}|^2 - V_0^2 > 2\,\beta_0. \tag{15}$$

Simulation: Velocity blow–up distance depends mainly on β_0;
Final velocity is greater for greater T_0.
Magnetic energy remains practically uniform over the distance.
$\beta_0(\mathbf{r}, t)$ goes up — the density fall (V–amplification) smoother.
Final velocities go up with $V_0[km/s] \sim d^{-1} V_{A0}$.
Flow with $3.3\,\mathrm{km/s}$ ends up with $\sim 100\,\mathrm{km/s}$ at $(Z - Z_0) \sim 0.09\,R_0$.

Flow Acceleration (N≠const) 1D

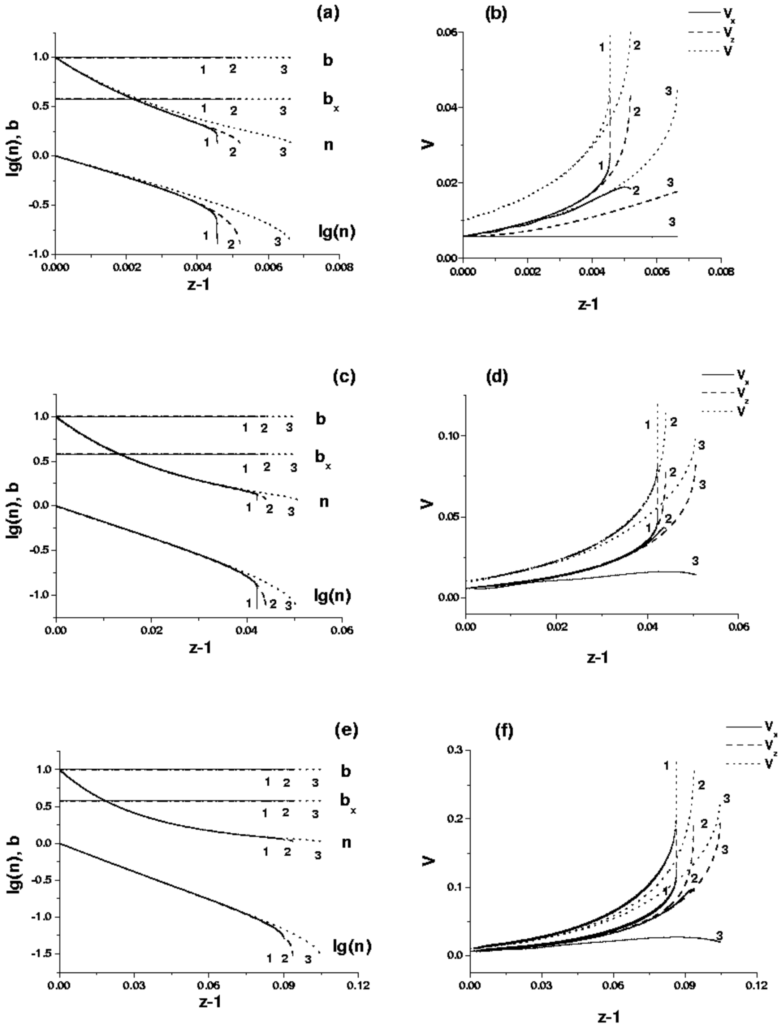

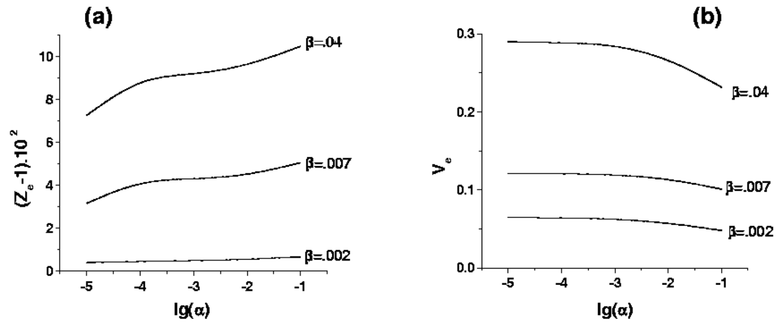

Sub-Alfvenic flows! Boundary conditions at:
***$Z_0>(1+2.8\bullet 10^{-3})R_s$* --- the influence of ionization can be neglected.**
$|b_0|=1$, $V_0=0.01V_{A0}$ (with $V_{x0}=V_{y0}=V_{z0}$)
DB parameters: *$d \sim a \sim 100$, $(a-d)/a^2 \sim 10^{-6}$*
Following are the (n_0; B_0; T_0; V_{A0}):
(a-b): 10^{12}cm^{-3}; 200G; 2eV; 440km/s; $\beta_0\sim0.002<<1$
(c-d): 10^{11}cm^{-3}; 100G; 5eV; 600km/s; $\beta_0\sim0.007<<1$
(e-f): 10^{11}cm^{-3}; 50G; 6eV; 330km/s; $\beta_0\sim0.04<1$

$|b|^2\sim$const; Density fall → velocity increase

3 Sets of curves labeled by α_0 for parameters versus height (Z-1). 1-2-3 correspond to: α_0=0.000013; 0.005; 0.1

Amplification is determined by local β_0

Let's rewrite DB equations in following way:

$$\alpha_0 \nabla \times \boldsymbol{b} = -\frac{1}{a}\,\boldsymbol{b} + n\,\boldsymbol{V}, \tag{16}$$

$$\alpha_0 \nabla \times \boldsymbol{V} = -\boldsymbol{b} + d\,n\,\boldsymbol{V}, \tag{17}$$

If *density fall* is at a much slower rate than the *slow scale* of the Beltrami system λ_- / α_0 (n – slowly varying - see Bernoulli condition: V^2, g – slowly varying), straightforward algebra gives:

$$\begin{pmatrix} \boldsymbol{Q}_+ \\ \boldsymbol{Q}_- \end{pmatrix} = \begin{pmatrix} \boldsymbol{b} - (\lambda_+ + a^{-1})\,\boldsymbol{V} \\ \boldsymbol{b} - (\lambda_- + a^{-1})\,\boldsymbol{V} \end{pmatrix} \tag{18}$$

each obeying its own independent (fully de–coupled) equation:

$$\nabla \times \boldsymbol{Q}_\pm = \frac{\lambda_\pm}{\alpha_0}\,\boldsymbol{Q}_\pm . \tag{19}$$

$\lambda_\pm = \frac{1}{2}[(d\,n - a^{-1}) \pm \sqrt{(d\,n + a^{-1})^2 - 4\,n}]$ are standard roots.

Mahajan et al. 2005, arXiv: astro-ph/0502345

The amplification conditions for flows

E.g. chromosphere: $a \sim d = 100$; $(a-d)/a\,d \sim 10^{-6}$. Restriction:

$$n \gg \frac{1}{a\,d} \tag{20}$$

— density fall is not more than 3 orders of magnitude, then

$$\lambda_+ \sim d\,n \qquad \lambda_- \sim \frac{a-d}{a\,d}. \tag{21}$$

Notice: for realistic parameters (chromosphere, TR, corona) $\alpha_0 \sim 10^{-9}$–10^{-11} and the fast Beltrami scale $\lambda_+/\alpha_0 \sim 10^{11} - 10^{13}$ is of no interest $\longrightarrow$ to a very oscillatory mode. Hence, we choose

$$\boldsymbol{Q}_+ = \boldsymbol{b} - (d\,n - a^{-1})\,\boldsymbol{V} \simeq \boldsymbol{b} - d\,n\,\boldsymbol{V} = 0, \tag{22}$$

and

$$\nabla \times \boldsymbol{Q}_- = \frac{a-d}{a\,d\,\alpha_0}\,\boldsymbol{Q}_- \tag{23}$$

$$\boldsymbol{Q}_- = \boldsymbol{b} - \frac{\boldsymbol{V}}{d} \simeq \boldsymbol{b}. \tag{24}$$

1D problem (Z along height, $b_0 = 1$ when normalized).
Eq.(22) leads to:

$$\frac{\partial b_x}{\partial z} = \frac{a-d}{a\,d\,\alpha_0}\; b_y, \qquad \frac{\partial b_y}{\partial z} = -\frac{a-d}{a\,d\,\alpha_0}\; b_x \tag{25}$$

implying:

$$\frac{\partial}{\partial z}\left(b_x^2 + b_y^2\right) = 0 \qquad \Longrightarrow \qquad b_x^2 + b_y^2 = b_{0\perp}^2. \tag{26}$$

Then, using eq.(22), one has:

$$V_x^2 + V_y^2 = \frac{b_{0\perp}^2}{d^2\, n^2}. \tag{27}$$

From Continuity Equation and DB condition one has:

$$V_z = \frac{V_{0z}}{n} \sim \frac{b_{0z}}{d\, n}. \tag{28}$$

Thus,

$$V^2 = \frac{1}{d^2\, n^2}. \tag{29}$$

Eq.(29) and Bernoulli condition ($T_0 = const$) lead to:

$$\left(-2\,\beta_0\, n^2 + \frac{1}{d^2}\right)\frac{\partial n}{\partial z} = n^3\, g. \tag{30}$$

Notice, that maximum allowed velocity for this mechanism is:

$$|V_{max}| = \frac{1}{d\, n_{min}} = (2\beta_0)^{1/2}. \tag{31}$$

Bernoulli condition reveals the origin of very fast first stage of dynamical acceleration observationally found (see simulation results).

Note: The analysis gave the same results for the varying temperature ($T = n^{-\mu}, \quad 0 < \mu < 1$).

Results for nonuniform density (analysis + simulation)

- The magnetic energy does not change much, $|b|^2 = const$ to leading order.
- There is a catastrophe in the system. When the velocity gets close to (31) the Eq.(30) becomes singular; the steep rise in velocity and code ceases to function (see comment later!)
- The distance over which the catastrophe appears is determined by the strength of gravity $g(z)$. As long as $2\,\beta_0\,n^2 > d^{-2}$, the $\partial_z n < 0$ and density decreases (velocity increases); rate depends on gravity.
- Eventual amplification of flow is determined by local β_0.
- α_0 to some extent is quite irrelevant, it just tells us how fast the transverse components of magnetic and velocity fields oscillate; it has little effect on the gross features of the system.

Comment: as the flows reach the blow–up distance the parameters cease to be slowly varying — the time–independent approach is no more valid. (For pressure pedestal theory see Guzdar et al. PoP 2005)

Reverse Dynamo – Macroscopic Fields Generation

Mahajan et al, 2005, ApJ 832, October 10

Fusion devices/Astrophysics - the emergence of macroscopic magnetic fields from an initially turbulent system.
Standard Dynamo - generation of macroscopic fields from (primarily microscopic) velocity fields.

The relaxations observed in the reverse field pinches is a vivid illustration of Dynamo in action. The Myriad phenomena in stellar atmospheres (heating, field opening, wind) impossible to explain without knowing the origin and nature of magnetic field structures.

Hall MHD: the velocity field is not specified externally (as in kinematic case) but **evolves in interaction with magnetic field**.

If short-scale turbulence $\rightarrow$ macroscopic magnetic fields, then under appropriate conditions the turbulence $\rightarrow$ macroscopic plasma flows.

The structures/magnetic elements produced by the turbulent amplification are destroyed/dissipated even before they are formed completely creating significant flows or leading to the heating (see Socas-Navarro & Manso Sainz (2005), Bellot Rubio eta al, 2001; Blackman 2005).

If the process of conversion of micro-scale kinetic energy to macro-scale magnetic energy is termed "dynamo" (D) then the mirror image process of the conversion of micro-scale magnetic energy to macro-scale kinetic energy could be called "reverse dynamo" (RD).

Uniform density case – incompressible flow.

α_0 is absorbed by choosing the normalizing length scale to be λ_{i0}. Gravity is ignored.

$$\frac{\partial \boldsymbol{B}}{\partial t} = \boldsymbol{\nabla} \times \left[[\boldsymbol{V} - \boldsymbol{\nabla} \times \boldsymbol{B}] \times \boldsymbol{B} \right], \qquad \boldsymbol{V}_e = \boldsymbol{V} - \boldsymbol{\nabla} \times \boldsymbol{B} \tag{32}$$

$$\frac{\partial \boldsymbol{V}}{\partial t} = \boldsymbol{V} \times (\boldsymbol{\nabla} \times \boldsymbol{V}) + (\boldsymbol{\nabla} \times \boldsymbol{B}) \times \boldsymbol{B} - \boldsymbol{\nabla} \left(P + \frac{V^2}{2} \right) \tag{33}$$

The total fields are broken into ambient fields and perturbations

$$\boldsymbol{B} = \boldsymbol{b}_0 + \boldsymbol{H} + \boldsymbol{b}$$

$$\boldsymbol{V} = \boldsymbol{v}_0 + \boldsymbol{U} + \boldsymbol{v}$$

$\boldsymbol{b}_0$, $\boldsymbol{v}_0$ - equilibrium; $\boldsymbol{H}$, $\boldsymbol{U}$ - macroscopic; $\boldsymbol{b}$, $\boldsymbol{v}$ - microscopic fields.

Equilibrium fields are taken to be the DB pair

obeying Bernoulli condition $\boldsymbol{\nabla}(p_0 + \boldsymbol{v}_0{}^2/2) = const$

$$\frac{\boldsymbol{b}_0}{a} + \boldsymbol{\nabla} \times \boldsymbol{b}_0 = \boldsymbol{v}_0, \quad \boldsymbol{b}_0 + \boldsymbol{\nabla} \times \boldsymbol{v}_0 = d\boldsymbol{v}_0, \tag{34}$$

which may be solved in terms of the SB fields $(\boldsymbol{\nabla} \times \boldsymbol{G}(\mu) = \mu \boldsymbol{G}(\mu))$

$$\boldsymbol{b}_0 = C_\lambda \boldsymbol{G}(\lambda) + C_\mu \boldsymbol{G}(\mu), \tag{35}$$

$$\boldsymbol{v}_0 = \left(a^{-1} + \lambda\right) C_\lambda \boldsymbol{G}(\lambda) + C_\mu \left(a^{-1} + \mu\right) \boldsymbol{G}(\mu). \tag{36}$$

$C_{\lambda/\mu}$ - arbitrary constants; a, d - set by invariants of equil. system.

Inverse scale lengths λ, μ are fully determined in terms of a, d (hence, initial helicities). As a, d vary, λ, μ can range from real to complex values of arbitrary magnitude.

Below: λ - micro-scale; μ - macro-scale structures..

Assumptions: $|b| \ll b_0$, $|v| < v_0$ at the same scale

Below $\boldsymbol{v}_{e0} \equiv \boldsymbol{v}_0 - \boldsymbol{\nabla} \times \boldsymbol{b}_0$

See for the details of closure model of Hall MHD Mininni et al, ApJ, 2003, 2005.

$$
\begin{aligned}
\partial_t \boldsymbol{U} = {} & \boldsymbol{U} \times (\boldsymbol{\nabla} \times \boldsymbol{U}) + \boldsymbol{\nabla} \times \boldsymbol{H} \times \boldsymbol{H} + \langle \boldsymbol{v}_0 \times (\boldsymbol{\nabla} \times \boldsymbol{v}) \\
& + \boldsymbol{v} \times (\boldsymbol{\nabla} \times \boldsymbol{v}_0) + (\boldsymbol{\nabla} \times \boldsymbol{b}_0) \times \boldsymbol{b} + (\boldsymbol{\nabla} \times \boldsymbol{b}) \times \boldsymbol{b}_0 \\
& - \langle \boldsymbol{\nabla}(\boldsymbol{v}_0 \cdot \boldsymbol{v}) \rangle - \boldsymbol{\nabla}\left(p + \frac{\boldsymbol{U}^2}{2}\right) \qquad (37)
\end{aligned}
$$

$$
\frac{\partial \boldsymbol{v}}{\partial t} = -(\boldsymbol{U} \cdot \boldsymbol{\nabla})\boldsymbol{v}_0 + (\boldsymbol{H} \cdot \boldsymbol{\nabla})\boldsymbol{b}_0 \qquad (38)
$$

$$
\frac{\partial \boldsymbol{b}}{\partial t} = (\boldsymbol{H} \cdot \boldsymbol{\nabla})\boldsymbol{v}_{e0} - (\boldsymbol{U} \cdot \boldsymbol{\nabla})\boldsymbol{b}_0 \qquad (39)
$$

$$
\frac{\partial \boldsymbol{H}}{\partial t} = \boldsymbol{\nabla} \times \langle [\boldsymbol{v}_e \times \boldsymbol{b}_0] + \boldsymbol{v}_{e0} \times \boldsymbol{b} \rangle + \boldsymbol{\nabla} \times [(\boldsymbol{U} - \boldsymbol{\nabla} \times \boldsymbol{H}) \times \boldsymbol{H}] \qquad (40)
$$

A closure model of the Hall MHD equations – general in two respects:

1) a closure of full set of equations – feedback of the micro-scale is consistently included in the evolution of $\boldsymbol{H}$, $\boldsymbol{U}$

2) role of the Hall current (especially in the dynamics of the micro–scale) is properly accounted.

Assumption: the original equilibrium is predominantly short-scale.

$$\boldsymbol{v}_0 = \boldsymbol{b}_0 \left(\lambda + a^{-1}\right) \tag{41}$$

leading to

$$\boldsymbol{v}_{e0} = \boldsymbol{v}_0 - \boldsymbol{\nabla} \times \boldsymbol{b}_0 = \boldsymbol{b}_0 \; a^{-1} \tag{42}$$

$$\dot{\boldsymbol{b}} = \left(a^{-1} \boldsymbol{H} - \boldsymbol{U}\right) \cdot \boldsymbol{\nabla} \boldsymbol{b}_0 \tag{43}$$

$$\dot{\boldsymbol{v}} = \left(\boldsymbol{H} - \left(\lambda + a^{-1}\right) \boldsymbol{U}\right) \cdot \boldsymbol{\nabla} \boldsymbol{b}_0 . \tag{44}$$

Limiting to "linear" treatment (initial acceleration state), neglecting nonlinear terms (that could play important role in saturation of macro-fields; *see comment later*):

$$\ddot{\boldsymbol{H}} \simeq \boldsymbol{\nabla} \times \left[\left(1 - \frac{\lambda}{a} - \frac{1}{a^2} \right) (H \cdot \boldsymbol{\nabla} \boldsymbol{b}_0) \times \boldsymbol{b}_0 \right], \tag{45}$$

$$\begin{aligned} \ddot{\boldsymbol{U}} &= \left(\lambda + \frac{1}{a} \right) \boldsymbol{\lambda} \dot{\boldsymbol{v}} - (\boldsymbol{\nabla} \times \dot{\boldsymbol{v}}) \times \boldsymbol{b}_0 \\ &\quad + (\boldsymbol{\nabla} \times \dot{\boldsymbol{b}} - \lambda \dot{\boldsymbol{b}}) \times \boldsymbol{b}_0 - \left(\lambda + \frac{1}{a} \right) \boldsymbol{\nabla} (\boldsymbol{b}_0 \cdot \dot{\boldsymbol{v}}). \end{aligned} \tag{46}$$

To compute spatial averages – isotropic ABC solution of SB system

$$
\begin{aligned}
b_{0x} &= \frac{b_0}{\sqrt{3}}\left[\sin\lambda y + \cos\lambda z\right] \\
b_{0y} &= \frac{b_0}{\sqrt{3}}\left[\sin\lambda z + \cos\lambda x\right] \\
b_{0z} &= \frac{b_0}{\sqrt{3}}\left[\sin\lambda x + \cos\lambda y\right].
\end{aligned}
$$

Calculating nonzero components, we arrive:

$$
\ddot{U} = \frac{\lambda}{2}\frac{b_0^2}{3}\boldsymbol{\nabla}\times\left[\left(\left(\lambda+\frac{1}{a}\right)^2\right)\boldsymbol{U}-\lambda\boldsymbol{H}\right] \tag{47}
$$

$$
\ddot{H} = -\lambda\frac{b_0^2}{3}\left(1-\frac{\lambda}{a}-\frac{1}{a^2}\right)\boldsymbol{\nabla}\times\boldsymbol{H}. \tag{48}
$$

where b_0^2 **measures the ambient micro scale magnetic energy** (also the kinetic energy because of (41)). The coefficients in these equations are determined by a and d ($\lambda = \lambda(a, d)$); to leading order, **$\boldsymbol{H}$ evolves independently of $\boldsymbol{U}$ but evolution of $\boldsymbol{U}$ does require knowledge of $\boldsymbol{H}$.**

Writing (47) and (48) formally as

$$\ddot{\boldsymbol{H}} = -r(\lambda)(\boldsymbol{\nabla} \times \boldsymbol{H}), \qquad \ddot{\boldsymbol{U}} = \boldsymbol{\nabla} \times [s(\lambda)\boldsymbol{U} + q(\lambda)\boldsymbol{H}], \tag{49}$$

Fourier analyzing

$$-\omega^2 \boldsymbol{H} = -i\, r\, (\boldsymbol{k} \times \boldsymbol{H}), \qquad -\omega^2 \boldsymbol{U} = -i\, k\, \times (s\boldsymbol{U} + q\boldsymbol{H}), \tag{50}$$

yielding the **growth rate** at which $\boldsymbol{H}$ and $\boldsymbol{U}$ increase,

$$\omega^4 = r^2 k^2 \qquad \omega^2 = -|r|(k). \tag{51}$$

Growing Macro-fields are related to one another as

$$\boldsymbol{U} = \frac{q}{(s+r)} \boldsymbol{H}. \tag{52}$$

A choice of a, d fixes relative amounts of microscopic energy in ambient fields $\longrightarrow$ in **the nascent macroscopic fields $\boldsymbol{U}$ or $\boldsymbol{H}$.**

Comment: the linear solution makes nonlinear terms strictly zero – it is an exact (a special class) solution of the nonlinear system and thus remains valid even as $\boldsymbol{U}$ and $\boldsymbol{H}$ grow to larger amplitudes (In MHD - nonlinear Alfvén wave: Walen 1944,1945; in HMHD - Mahajan & Krishan, MNRAS 2005).

(i) $a \sim d \gg 1$, inverse micro scale $\lambda \sim a \gg 1 \Longrightarrow \boldsymbol{v}_0 \sim a\,\boldsymbol{b}_0 \gg \boldsymbol{b}_0$, i.e, the ambient micro-scales fields are primarily kinetic.

Generated macro-fields have opposite ordering, $\boldsymbol{U} \sim a^{-1}\boldsymbol{H} \ll \boldsymbol{H}$.

An example of the straight **dynamo mechanism** – super-Alfvénic "turbulent flows" lead to steady flows that are equally sub–Alfvénic.

Important: the dynamo effect must always be accompanied by the generation of macro-scale plasma flows.

This realization can have serious consequences for defining the initial setup for the later dynamics in the stellar atmosphere. The presence of an initial macro-scale velocity field during the flux emergence processes is, for instance, always guaranteed by the mechanism exposed above.

Implication: all models of chromosphere heating / flow acceleration should take into account the existence of macro-scale primary plasma flows (even weak) and their self-consistent coupling.

(ii) $a \sim d \ll 1$ the inverse micro scale $\lambda \sim a - a^{-1} \gg 1 \Longrightarrow$ $\boldsymbol{v}_0 \sim a\, \boldsymbol{b}_0 \ll \boldsymbol{b}_0$. **The ambient energy is mostly magnetic.** Photo-spheres/chromospheres: turbulent velocity field may exist, but turbulent magnetic field is dominant.

Micro-scale magnetically dominant initial system creates macro-scale fields $\boldsymbol{U} \sim a^{-1}\boldsymbol{H} \gg \boldsymbol{H}$ that are kinetically abundant.
Starting from a strongly sub-Alfvénic turbulent flow, system generates a strongly super-Alfvénic macro–scale flow – **"reverse dynamo":** in the region of a given astrophysical system where the fluctuating/turbulent magnetic field is initially dominant, the magneto-fluid coupling induces efficient/significant acceleration and part of the magnetic energy will be transferred to steady plasma flows.

Product of the "reverse dynamo" mech.: – a steady super–Alfvénic flow; a macro flow accompanied by a weak magnetic field.
(compare with Blackman & Field, PoP 2004 for a magnetically driven "inverse dynamo"; magnetic field growth on much larger scales, and significant velocity fluctuations with finite volume averaged kinetic helicity are found).
RD → observations: fast flows are found in weak field regions (Woo et al, ApJ, 2004).

Results:

- **Dynamo and "Reverse Dynamo" mechanisms** have same origin – **are manifestation of magneto-fluid coupling**;

- $\boldsymbol{U \sim H}$ **implies: they must be present simultaneously**.

  Greater the macro-scale magnetic field (generated locally), greater the macro-scale velocity field (generated locally);

- **Growth rate of macro-fields** is defined by DB parameters (by ambient magnetic and generalized helicities) and **scales directly with ambient turbulent energy** $\sim b_0^2 \ (v_0^2)$.

  Larger the initial turbulent magnetic energy, stronger the acceleration of the flow.

  Impacts: on the evolution of large-scale magnetic fields and their opening up with respect to fast particle escape from stellar coronae; on the dynamical and continuous kinetic energy supply of plasma flows observed in astrophysical systems.

  Initial and final states have finite heliciies (magnetic and kinetic). The helicity densities are dynamical parameters that evolve self-consistently during the flow acceleration.

A simulation Example for Dynamical Acceleration

2.5D numerical simulation of the general two-fluid equations in Cartesian Geometry. Code: Mahajan et al. PoP 2001, Mahajan et al, 2005, arXiv: astro-ph/0502345

Simulation system contains:

- an ambient macroscopic field
- effects not included in the analysis:
    1. dissipation and heat flux
    2. the vorticity and the Hall terms
    3. plasma is compressible embedded in a gravitational field $\rightarrow$ extra possibility for micro-scale structure creation.

Transport coefficients are taken from Braginskii and are local.

Diffusion time of magnetic field > duration of interaction process (would require $T \leq$ a few eV-s).

Trapping and amplification of a weak flow impinging on a single closed-line structure. Choice of initial conditions is guided by the observational evidence of the self-consistent process of acceleration and trapping/heating of plasma in the finely structured solar atmosphere (e.g. Aschwanden et al. 2001, Woo et al. 2004)

Weak symmetric up-flow:

Initially Gaussian; peak is located in the central region of a single closed magnetic field structure.

$|\mathbf{V}|_{0max} \ll C_{s0}$ C_{s0} - initial sound speed.

The initial velocity field is pulse-like; time duration - $t_0 = 100\,s$.

The magnetic field:

$\mathbf{B} = \nabla \times \mathbf{A} + B_z\,\hat{\mathbf{z}}$ $\mathbf{A}(0; A_y; 0)$; $\mathbf{b} = \mathbf{B}/B_{0z}$; $b_x(t, x, z \neq 0) \neq 0$.

Field maximum $B_{0z} = 100\,G$ - initially uniform it time.

Initial and boundary flow parameters:

$V_{0max}(x_o, z = 0) = V_{0z} = 2.18{\cdot}10^5\,cm/s$; $n_{0max} = 10^{12}\,cm^{-3}$; $T(x, z = 0) = const = T_0 = 10\,eV$.

The background plasma density: $n_{bg} = 0.2 n_{0max}$.

Simulations: $n(x, z, t = 0) = n/n_{0max}$ - an exponentially decreasing function of z.

Boundary condition: $\partial_x \mathcal{K}(x = \pm\infty, z, t) = 0$ - with sufficiently high accuracy for all parameters $\mathcal{K}(\mathbf{A}, T, \mathbf{V}, \mathbf{B}, n)$.

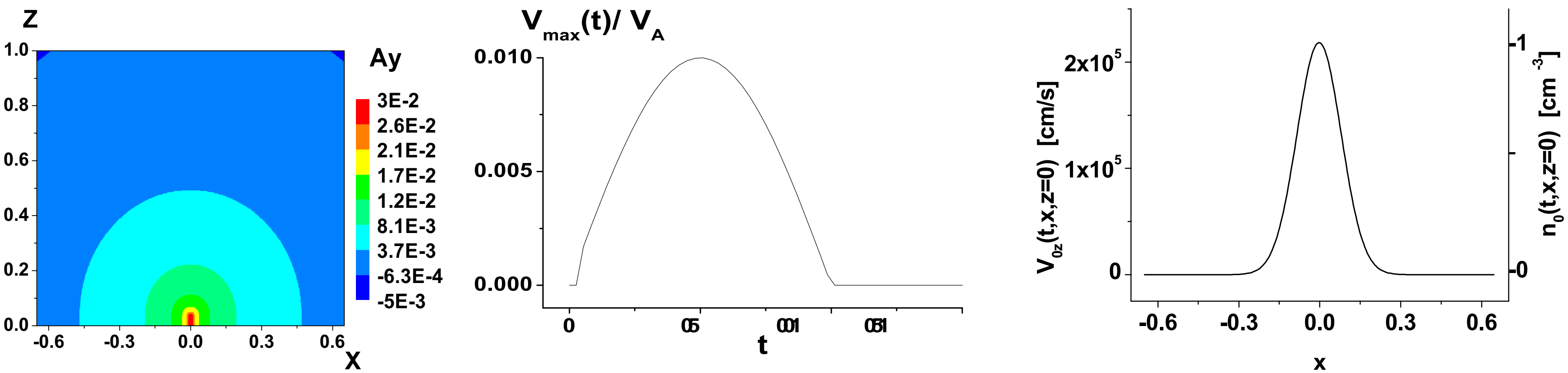
Z
1.0
0.8
0.6
0.4
0.2
0.0
-0.6
-0.3
0.0
0.3
0.6
X
Ay
3E-2
2.6E-2
2.1E-2
1.7E-2
1.2E-2
8.1E-3
3.7E-3
-6.3E-4
-5E-3
V_max(t)/ V_A
0.010
0.005
0.000
0
t
2x10^5
1x10^5
0
V_0z(t,x,z=0) [cm/s]
n_0(t,x,z=0) [cm^-3]
1
0
-0.6
-0.3
0.0
0.3
0.6
x

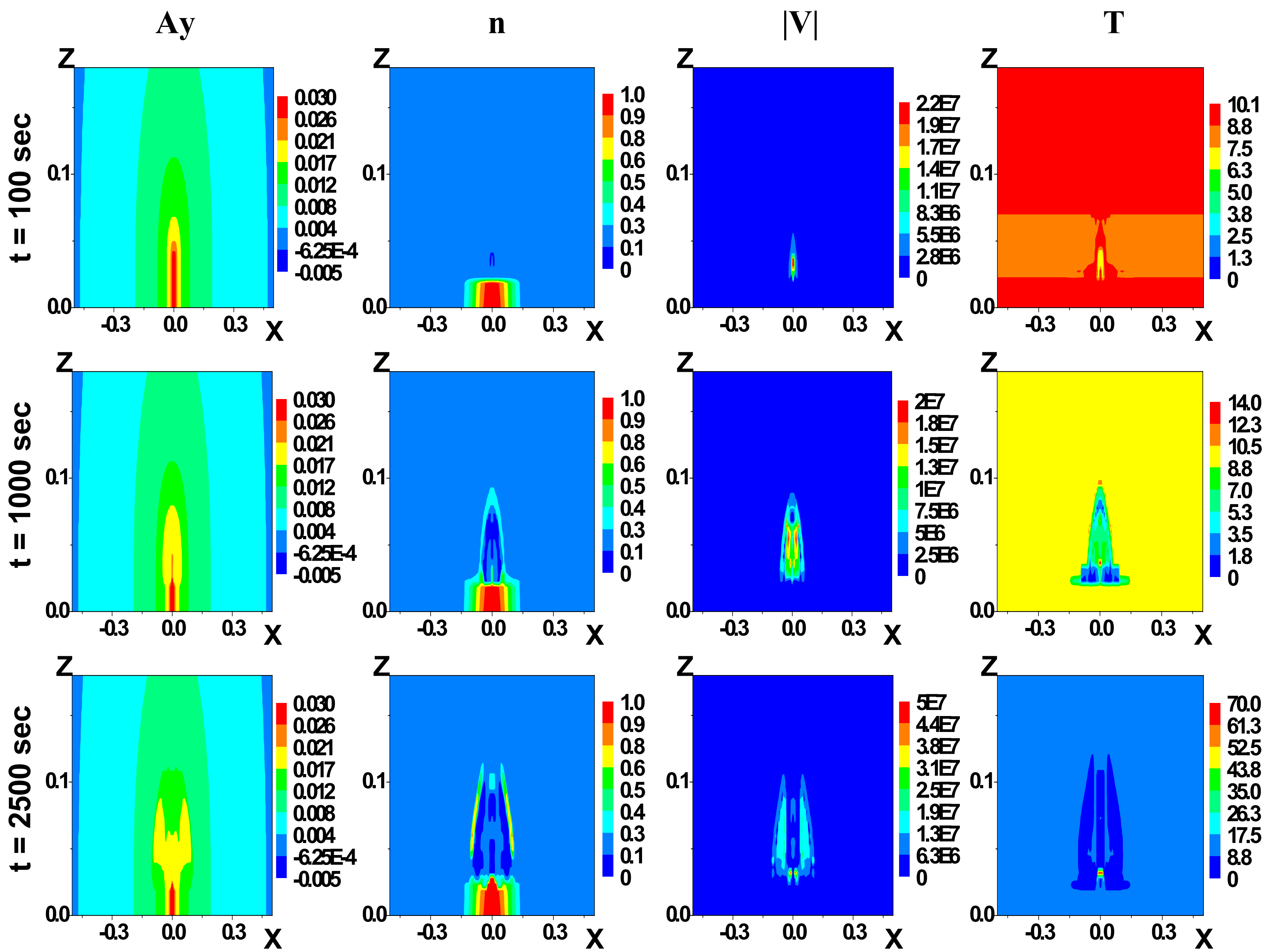

Ay
n
|V|
T
t = 100 sec
t = 1000 sec
t = 2500 sec
Z
X
0.1
0.0
-0.3
0.0
0.3
0.030
0.026
0.021
0.017
0.012
0.008
0.004
-6.25E-4
-0.005
1.0
0.9
0.8
0.6
0.5
0.4
0.3
0.1
0
2.2E7
1.9E7
1.7E7
1.4E7
1.1E7
8.3E6
5.5E6
2.8E6
0
10.1
8.8
7.5
6.3
5.0
3.8
2.5
1.3
0
2E7
1.8E7
1.5E7
1.3E7
1E7
7.5E6
5E6
2.5E6
0
14.0
12.3
10.5
8.8
7.0
5.3
3.5
1.8
0
5E7
4.4E7
3.8E7
3.1E7
2.5E7
1.9E7
1.3E7
6.3E6
0
70.0
61.3
52.5
43.8
35.0
26.3
17.5
8.8
0

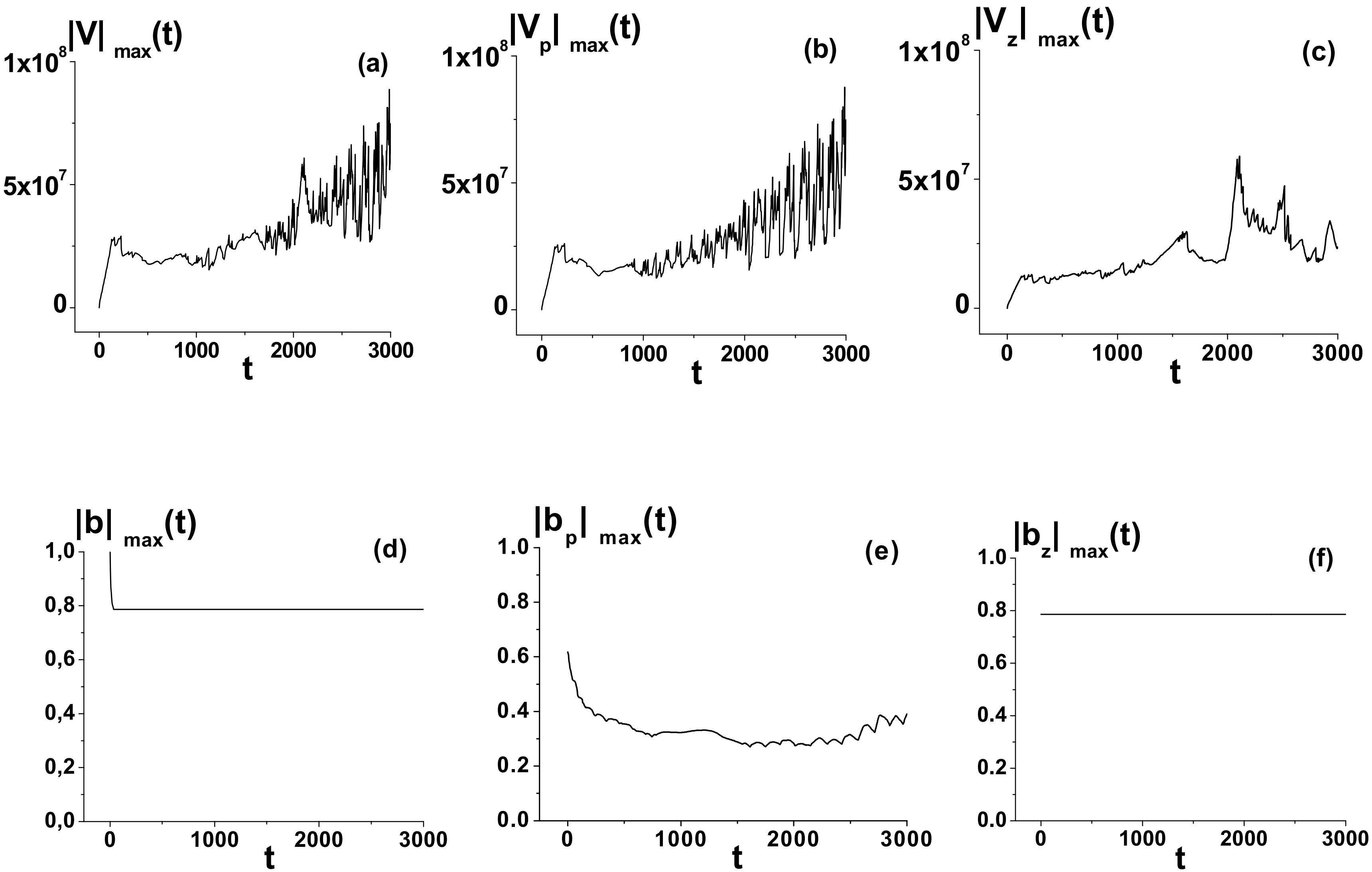

|V| max(t)
(a)
1x10^8
5x10^7
0
0
1000
2000
3000
t
|Vp| max(t)
(b)
1x10^8
5x10^7
0
0
1000
2000
3000
t
|Vz| max(t)
(c)
1x10^8
5x10^7
0
0
1000
2000
3000
t
|b| max(t)
(d)
1,0
0,8
0,6
0,4
0,2
0,0
0
1000
2000
3000
t
|bp| max(t)
(e)
1.0
0.8
0.6
0.4
0.2
0.0
0
1000
2000
3000
t
|bz| max(t)
(f)
1.0
0.8
0.6
0.4
0.2
0.0
0
1000
2000
3000
t

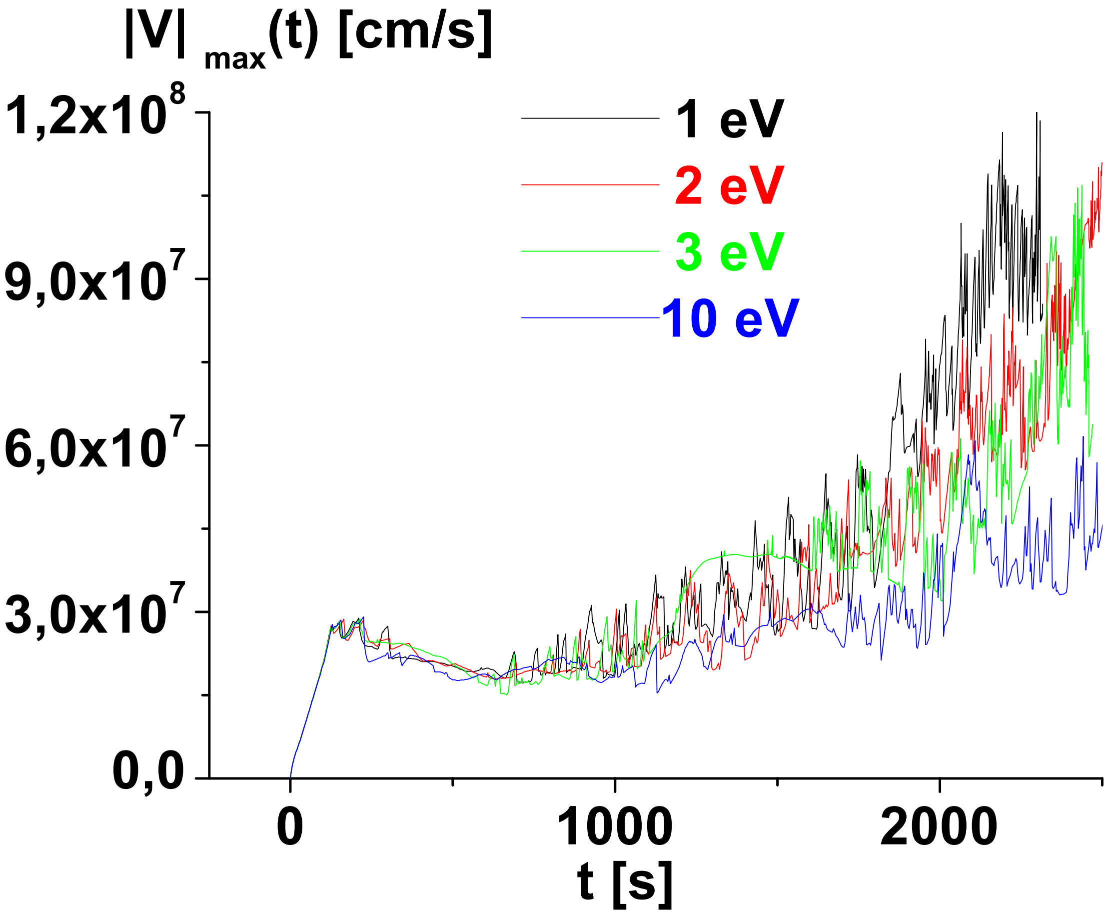

Acceleration of flows for different initial temperature - Controlling effect of T_0 and B_0.

(1) Acceleration is significant in the vicinity of magnetic field-maximum (originally present or newly created during the evolution) with strong deformation of field lines + energy re-distribution due to MFC+dissipation.

(2) Initially, a part of flow is trapped in the maximum field localization area, accumulated, cooled and accelerated. The accelerated flow reaches speeds greater than 100 km/s in less than 100 s (observations).

(3) After this stage the flow passes through a series of quasi-equilibria. In this relatively extended era ($\sim 1000\, s$) of stochastic/oscilating acceleration, the intermittent flows continuously acquire energy.

(4) The flow starts to accelerate again (consistent with the analytical prediction): acceleration is highest in strong field regions (**newly generated!**).

Accelerated daughter flows (macro-scale) are decoupled from mother flow carrying currents, modifying initial arcade field creating new b_{max} localization areas at $\sim 0.01\, R_s$ from interaction surface.

(5) **Controlling effects of initial T_0 and B_0 are explored**.

- Dissipation present: Hall term ($\sim \alpha_0$) (through the mediation of micro-scale physics) plays a crucial role in acceleration/heating processes. Existence of initial fast acceleration in the region of maximum localization of original magnetic field, and the creation of new areas of macro-scale magnetic field localization with simultaneous transfer of the magnetic energy (oscillatory, micro-scale) to flow kinetic energy are manifestations of the combined effects of the dynamo and inverse dynamo phenomena.
- The maintenance of quasi-steady flows for rather significant period is also an effect of the continuous energy supply from fluctuations (due to the dissipative, Hall and vorticity effects). These flows are likely to provide a very important input element for understanding the finely structured atmospheres with their richness of dynamical structures as well as for the mechanisms of heating, field opening and possible escape of plasmas.
- Simulation: **actual h_1, h_2 - dynamical**. Even if they are not in the required range initially, their evolution could bring them in the range where they could satisfy conditions needed to efficiently generate flows. Explantion of several phases of acceleration. Dissipation effects - fundamental role in setting up these distinct stages (modifying generalized vorticity → modification of field-lines, creation of micro scales (shocks, fast fluctuations)).